Co-published by
Institute of Fluid-Flow Machinery
Polish Academy of Sciences
Committee on Thermodynamics and Combustion
Polish Academy of Sciences

http://www.imp.gda.pl/archives-of-thermodynamics/

Thermal analysis of acetone and water in closed loop pulsating heat pipe

Haider Ali[a], Muhammad Amjad[a], Muhammad Ishaq[a], Mohammed Marshad R. Alharbi[b], Krzysztof Kędzia[c], Ahmed Zubair Jan[c*]

[a]Department of Mathematics, COMSATS University Islamabad, Vehari Campus, Vehari 61100, Pakistan
[b]Ministry of Education, Saudi Arabia
[c]Faculty of Mechanical Engineering, Wroclaw University of Science and Technology, Wroclaw, Poland
*Corresponding author email: ahmed.jan@pwr.edu.pl

Received: 08.12.2023; revised: 23.06.2024; accepted: 29.10.2024

Abstract

Thermal conductivity and transition are the two stages of a closed loop pulsating heat pipe's operation. A device called a closed loop pulsating heat pipe transfers heat at various heat inputs. The thermal performance of the closed loop pulsating heat pipe is impacted by various types of modifications. Heat transfer characteristics of the closed loop pulsating heat pipe are to be observed using computational fluid dynamics analysis. The aim of this study is to improve the heat conductivity of the closed loop pulsating heat pipe with the changing filling ratio. This study presents the closed loop pulsating heat pipe modeling by using ANSYS Workbench. ANSYS Fluent is considered to model the above stated phenomenon and computational fluid dynamics simulations are performed for different variations of temperature and filling ratio. The model is analyzed at 200W−300W heat flux for 100−400 iterations and the vaporized form is obtained. The temperature and iterations variations are the key parameters of the study. It is concluded that the temperature of the evaporator increased more at different levels of time as compared to the temperature of the condenser. In this analysis, by giving different heat inputs and evaporator sections, the heat flux in the condenser section is observed. It is concluded that the time and heat flux are the most affecting parameters in this study.

Keywords: Heat transfer; Closed loop pulsing heat pipes; Thermal analysis; ANSYS workbench; Computational fluid dynamics

Vol. 46(2025), No. 2, 29–37; doi: 10.24425/ather.2025.154917

Cite this manuscript as: Ali, H., Amjad, M., Ishaq, M., Alharbi, M.M.R., Kędzia, K., & Jan, A.Z. (2025). Thermal Analysis of Acetone and Water in Closed Loop Pulsating Heat Pipe. *Archives of Thermodynamics*, 46(2), 29−37.

1. Introduction

An effective method of transferring heat between hot and cold sources is a closed loop pulsing heat pipe (CLPHP). An oscillating pulsating heat pipe (PHP) is another name for a pulsating heat pipe. CLPHP is in thermal contact with the condenser section from one side which is the end of the tube and the other is the evaporator section. After providing heat to the evaporator, the condenser section oscillates with liquid plugs and vapour bubbles. The plugs alternate between hot and cold regions.

CLPHPs are powerful heat transfer innovations with high thermal performance. The idea of CLPHP was introduced by Akachi [1] in 1990. PHP has been designed so that heat moves

Nomenclature

c – specific heat, J/(kg·K)
D – diameter of CLPHP, m
f – surface tension, N/m
k – Boltzmann constant, J/K
p – pressure, N/m^2
T – temperature, K
u – velocity, m/s

Greek symbols

μ – dynamic viscosity, Pa·s
ρ – density, kg/m^3
σ – vapour-liquid surface tension coefficient, N/m

Subscripts and Superscripts

g – gas
l – liquid

Abbreviations and Acronyms

CLPHP – closed loop pulsating heat pipe
CFD – computational fluid dynamics
PHP – pulsating heat pipe
VOF – volume of fluid (method)

fluid. CLPHP must have two portions: heat receiving and radiating portions. PHP is a technology that transfers heat in the condenser area and gets it from the evaporator section. The flow of fluid and vapour is formed and a capillary action is formed.

Suresh and Bhramara [2] performed computational fluid dynamics (CFD) analysis of a single-turn PHP by using Ansys CFX. They considered different filling ratios of 60%, 70% and 80% and found a 60% filling ratio to be the best choice under different conditions. They concluded and suggested that a 60% filling ratio shows better heat transfer characteristics.

To attain the alternating vapour-liquid state, the PHP diameter must satisfy specific criteria. So, a formula was presented by Wang et al. [3] to measure the allowable inner diameter of PHP:

$$0.7\sqrt{\frac{\sigma}{(\rho_l-\rho_g)g}} \leq D \leq 2\sqrt{\frac{\sigma}{(\rho_l-\rho_g)g}}.$$

From the above equation, it can be noted that the surface tension has a great impact on the inner diameter of a closed-loop PHP.

Reddy et al. [4] analysed the thermal performance of ethanol and distilled water experimentally with a filling ratio of 50%. They used copper to construct PHP and the inner diameter was considered to be 2 mm. They concluded that the thermal performance of ethanol is finer than that of distilled water. Girish et al. [5] considered acetone, ethanol and methanol as working fluids in the analysis of CLPHP. Different heat inputs from 7 W to 15 W with filling ratios from 60% to 80% were considered. By increasing the heat coefficient of working fluids, the thermal resistance was reduced. Among all the considered working fluids, Acetone produces good results with a heat input of 13 W and a 60% filling ratio. Rudresha et al. [6] performed the CFD analysis of water and ethylene alcohol by utilizing Ansys. They concluded that the surface tension and thermal performance of water are better than those of the ethylene alcohol at the 60% filling ratio.

Betancur et al. [7] investigated PHP in a vertical position with various heat power inputs. A copper tube was utilized with five U-turns, 10 channels of planner serpentine, and an external and internal diameter of 4.76 mm and 3.18 mm, respectively. The thermal performance and flow along the tube were examined. Distilled water with a 50% filling ratio was considered as the working fluid and it was deduced that the motion of flow was reduced as a result of hindrance in the liquid film creation caused by the superhydrophobic coating.

Li and Li [8] analysed the application of PHP in high-performance central processing units (CPUs). Numerous high-power CPUs are utilized in data centres, which leads to the production of heat. They examined the whole research on CLPHP and different factors affecting the performance of PHP. The system's processor, storage, power supply, chip and voltage regulator are heat-generating components. Their research guided future research and engineering applications. The thermal performance of CLPHP was examined by Haque et al. [9] experimentally and by performing CFD simulations in Ansys. They considered the acetone-acetone vapours for this analysis. They calculated the thermal coefficient using the thermocouple temperature distribution. The CLPHP was built of copper, with a diameter of 1.95 mm and a total length of 540 mm. Different heat inputs were considered. They concluded that the increased heat transfer coefficient, reduced thermal resistance and heat transfer properties of CLPHP gave a good performance at a filling ratio of 60%.

Xue and Qu [10] used the high-speed camera to investigate the connection between PHP thermos hydrodynamics and flow patterns. In PHP, ammonia was utilized as a working fluid. PHP was made of quartz glass and had 6 turns and the outer diameter and inner diameter were considered to be 6 mm and 2 mm, respectively. The filling ratio was considered to be 70% with different heat inputs from 25 W to 250 W. They described the influence of vapour plugs, liquid slugs and also the velocity of the vapour. Pachghare and Mahalle [11] experimentally analysed the thermal performance of CLPHP. CLPHP was constructed of copper, having external and internal diameters of 3.6 mm and 2 mm, respectively. Different heat inputs were given from 10 W to 100 W and the filling ratio was fixed at 50% for all the experiments. The length of the adiabatic section, evaporation section and condenser section was kept at 50 mm. Water, ethanol, methanol, acetone and certain binary mixtures were assumed to be working fluids for this experiment. They concluded that a crucial factor for the thermal performance of CLPHP is the operating fluid, and acetone gave the best results among all the working fluids assumed.

Due to higher heat flux dissipation, electronic components' efficiency and performance have improved. Many devices have proved to be useful in microelectronic thermal management. In this field (thermal management of electronics), PHP cooling was an emerging and new technique. Baitule and Pachghare [12] used this technique to analyse the thermal performance of

CLPHP experimentally. The internal and external diameters of the copper-based evaporator and condenser portion were assumed to be 2 mm and 3 mm, respectively. The whole length of CLPHP was 1080 mm and the analysis was done on vertical surfaces with various heat loads ranging from 10 W to 100 W with a gap of 10 W per step. Acetone, methanol, water and ethanol were tested in CLPHP as working fluids for different filling ratios from 0% to 100% with a gap of 20% in each step. The results depicted that a lower thermal resistance, heat transfer characteristics, and greater CLPHP heat transfer coefficient produced superior results for various heat inputs at a 60% filling ratio. Patel and Mehta [13] investigated the thermal performance of 9-turn CLPHP. The inner and outer diameters were assumed to be 2 mm and 4 mm respectively. The lengths of the adiabatic, evaporator and condenser sections were considered 100 mm, 40 mm, and 50 mm, respectively. Throughout the trial, the working fluid was water, with a fixed filling ratio of 50%. Evaporator heaters were positioned in various orientations, including horizontal (90^0), vertical top (180^0), and bottom (0^0), as well as the inclined top (135^0) and bottom (45^0), to study the gravitational effect. The heat input ranged from 10 W to 50 W. The outcomes showed how gravity and input heat flux affected the thermal efficiency of CLPHP. From this perspective, Yeswanth and Bhaskara Rao [14] manipulated the geometry to investigate the thermal performance of a single-loop closed PHP. Geometry was modified by changing the surface area on the condenser side. To enhance the capacity for heat transfer, the best geometry was discovered. Rahman et al. [15] experimentally investigated the thermal efficiency of CLPHP with and without fins. Water and acetone were taken as working fluids for both cases. The values of the filling ratio were taken as 40%, 50%, 60% and 70%. The values of the angle of inclination were considered to be 0^0, 30^0, 45^0 and 60^0 and the heat input was taken from 10W to 100W in the stages of 10W. CLPHP was constructed from a copper tube, and its inner and outer diameters were assumed to be 2mm and 3mm, respectively. The results depicted that better results were observed for acetone and water for the 70% and 50% filling ratio, respectively, at an inclination angle of 0^0 for both cases.

Pachghare and Mahalle [16] experimentally analysed the copper-made CLPHP having an internal and external diameter of 2 mm and 3.6 mm, respectively. Water-methanol, water-ethanol and water-acetone binary mixtures were chosen as the working fluids. The distances of the adiabatic, evaporator and condenser sections were considered 170 mm, 42 mm and 50 mm, respectively, using a fixed filling ratio. The findings showed that the thermal resistance reduced gradually up to a heat input of 40 W and thereafter became reasonably stable. It was concluded that water-acetone gave the best results in comparison to the other considered fluids. Sree et al. [17] used CFD to examine the influence of several parameters on the thermal performance of CLPHP. Water was used as the working fluid, and CLPHP was manufactured with internal diameters of 2 mm and outer diameters of 3 mm. Different heat inputs were taken which were 16 W, 32 W and 48 W. The temperature, liquid volume fractions and pressure variations between three portions of CLPHP were described for various assimilations of the geometry of CLPHP, and the experimental and CFD results of thermal performance were compared. Yang et al. [18] analysed the operational limitation of CLPHP which was made up of 40 copper tubes with internal diameters of 1 mm and 2 mm, and the filling ratios were 30%, 50% and 70%. In the analysis, the effect of filling ratio, different heat inputs, operational orientation and inner diameter was calculated. They concluded that the inner diameter of 2mm gave the best results as compared to 1mm and also the 50% filling ratio was ideal in both cases.

PHP has gained great attention from theoretical and experimental research in recent times. Khandekar et al. [19] gave further visualization results to emphasize the complexity of the mathematical formulation of the modelling challenge. The results included a thorough analysis of the CLPHP modelling methodologies currently in use. The significant challenges that were embroiled in the modelling of such devices were thoroughly examined. It was uncommon to see a combination of such mechanisms and events, such as flooding or bridging, bubble agglomeration and changes in flow regime, bubble nucleation and collapse, pumping action, temperature, pressure and non-equilibrium conditions. They concluded that each of these factors affects well how a gadget conducts heat. The attempts to characterize the device in terms of controllable thermomechanical boundary conditions and a basic problem were made by Khandekar and Groll [20].

For CLPHPs, Xu et al. [21] offered the visualization with high-speed flow findings that showed that there is a bulk circulation flow that is long-lasting and shifts the direction of flow. The sine oscillation waves were visible. However, the local oscillating waves were overlaid and had brief periods and modest oscillation amplitudes. They concluded that the oscillation flow in PHP was caused by the sophisticated coupled effects of coalescence, bubble nucleation and condensation.

Khan and Nadeem [22] explored the heat and mass transfer for Maxwell nanofluid and concluded that the time relaxation parameter is one of the key parameters in this case. Khan et al. [23] investigated the ternary hybrid nanomaterials and noted that the slip parameter and Darcy-Forchheimer parameter were the key parameters in this study. Fourier's heat flux model was implemented by Khan et al. [24] to compute the heat transfer rate of a micropolar fluid. They observed an enhancement in heat transfer with an increment in the micro-polar parameter. Some other latest articles in this field are presented in the reference list as [24−29]. Ju et al. [30] provided information about the stability of oil droplets by varying certain parameters. Khan et al. [31] considered the Casson nanomaterials to compute the entropy generation numerically and the impact of inclusive parameters. Khan et al. [32] depicted that the Soret and Dufour numbers are the key parameters in analysing the Maxwell fluid. Tian et al. [33] experimentally studied the heat transfer phenomena due to electric fields and macro-structured surfaces during electrospray cooling. Khan et al. [34] modelled the partial differential equations for microelectromechanical systems and performed the stability analysis by employing the homotopy perturbation method. Khan et al. [35] depicted that the Yamada-Ota

model has proficient outcomes in comparison to the Xue model for heat exchangers.

The existing literature includes the experimental results of these types of models leaving a gap for CFD simulations. In the current study, the thermal performance of CLPHP will be analysed using the Ansys 2021 R2. Acetone, acetone vapours and water are taken as working fluids which were not considered for this specific case before. Due to this consideration, the numerical results will be established and these will be useful in validating the results experimentally.

2. Materials and methods

2.1. Governing equations

For a two-phase flow, the gas-liquid interaction is recognized as the volume of fluid (VOF). The general method to model such flow utilizing a sole fluid creation based on the VOF method is pursued for shaping the slug in the capillaries. This phenomenon could be expressed using the following equations:

$$\nabla \cdot \vec{u} = 0,$$

$$\frac{\partial(\rho\vec{u})}{\partial t} + \nabla \cdot (\overrightarrow{u} \cdot \rho\vec{u}) = -\nabla p + \nabla \cdot [\mu(\nabla\vec{u} + (\nabla\vec{u})^T)] + \overrightarrow{f_\sigma},$$

$$\frac{\partial(\rho c T)}{\partial t} + \nabla \cdot (\rho c \vec{u} T) = \nabla \cdot (k \nabla T),$$

where $\vec{u}, \rho, \mu, p, T, k, \overrightarrow{f_\sigma}$ and c are the velocity vector, density, dynamic viscosity, pressure, temperature, thermal conductivity, surface tension and specific heat, respectively. The above stated equations are solved utilizing the VOF method.

The CLPHP filling ratio is taken to be 70%. Water and acetone are the operating fluids, and the internal and external dimensions are 2 mm and 3 mm, respectively. The size of the evaporator, condenser and adiabatic section is considered to be 116 mm, 53 mm, and 50 mm, respectively. The heat flux is given as 200W. The model of a two-turn PHP is designed in Ansys Fluent software. In this analysis, the temperature difference is to be determined between the condenser and evaporator.

2.2. CFD simulation

This study aims to analyse the thermal performance of CLPHP with the variations in the evaporator section under load conditions using acetone, acetone vapours, and water as working fluids. This simulation is made in CFD software ANSYS 2021 R2.

Also, the flow paradigm of the above-stated working fluids inside the CLPHP is to be noted to suggest the trajectory. Furthermore, the temperature differences in the condenser and evaporator are considered performance parameters.

2.2.1. Methodology

Based on the literature cited above, the article by Giri and Pachghare [36] is considered to define the basic parameters. This article was restricted to only a few conditions. In this study, it is extended to certain variations in different parameters. CFD analysis is performed using certainly suitable schemes and the simulation is performed until the achievement of the required convergence criterion.

2.3. Geometry and meshing

The work of Giri and Pachghare [36] is considered to construct the basic geometry. The grid-independent test is performed for each model and the solution is also independent of the mesh resolution.

2.3.1. Geometry

The CLPHP is designed in ANSYS workbench. CLPHP is based on three sections: the evaporation section, the adiabatic section, and the condenser section which are shown in Figs. 1, 2 and 3, respectively. The copper domain is not deemed in the modelling of geometry. Only the fluid domain is under consideration in this case. Dimensions of CLPHP are demonstrated below in Table 1.

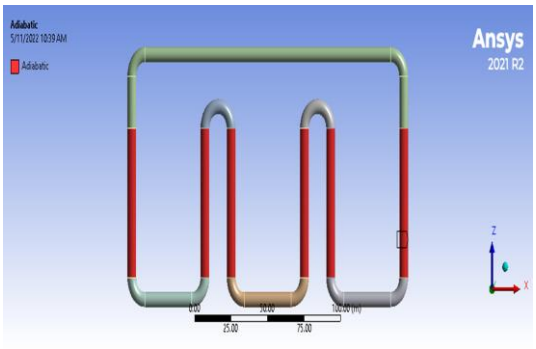

Fig. 1. Adiabatic section.

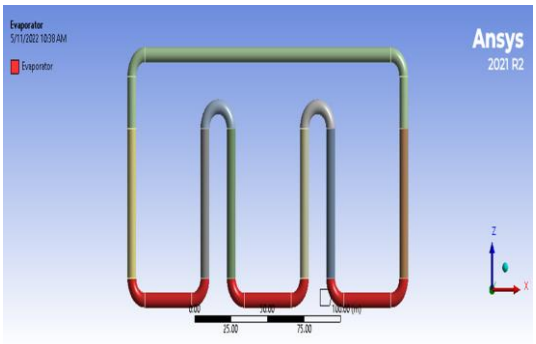

Fig. 2. Evaporator section.

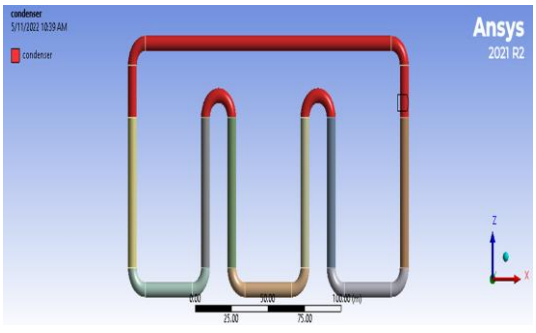

Fig. 3. Condenser section.

Table 1. Details of CLPHP geometry.

Specifications	Dimensions
Inner diameter	3 mm
Outer diameter	5 mm
Evaporator section length	116 mm
Condenser section length	53 mm
Adiabatic section length	50 mm

2.3.2. Meshing

A mesh is a grid that is made of points and cells. In the meshing, complex geometries are divided into elements. It depends on the shape of the geometry. When the geometry area is larger, more cells are created, which means the calculations take longer time. On the other hand, if the geometry area is smaller, fewer cells are created, so the calculations take less time. Meshing allows us to visualize the flow pattern inside the tube. Creating more cells improves the accuracy of the results, while fewer cells lead to less precise outcomes. In this analysis, we used a cell size of 0.3 mm. Near the walls, we made the mesh elements smaller to ensure better accuracy in capturing details close to the outer walls of the CLPHP The number of nodes and number of elements in the generated mesh are 384 438 and 453 381, respectively. The section of CLPHP with water vapour is shown in Fig. 4. In this analysis, the filling ratio of CLPHP is taken at 70% which is shown in Fig. 5. This meshing process is done by using the ANSYS Fluent. The working fluid is considered water and acetone.

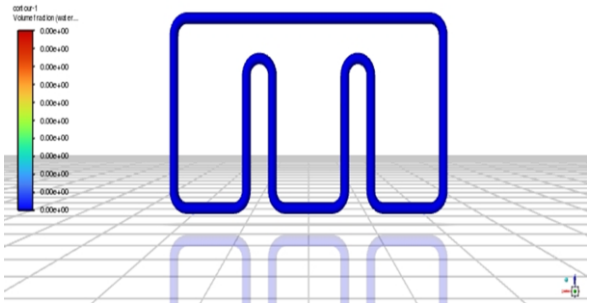

Fig. 4. CLPHP with vapour.

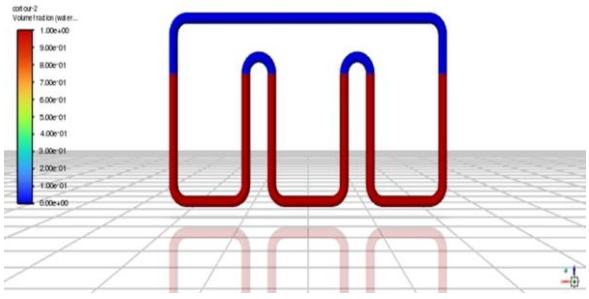

Fig. 5. CLPHP with a mixture of fluids.

2.4. Analysis settings

The steady-state analysis is conducted in Fluent although a major part of the thermal analysis with the phenomena of phase change is primarily a transient case. The analysis is performed to confirm the state of the fluid whether it is steady-state or transient. The variation between a steady-state simulation and its transient solution is that this simulation neglects much of the cross and higher-order terms. These terms all approach zero in a steady state, exerting minimal influence on the outcome. Similarly, transient simulations encompass all these terms. Generally, this implies that the aforementioned model has a better convergence as fewer terms have to be modelled and some transient non-linearity is neglected. For some specific cases, this leads to convergence.

In this section, the mesh is checked. To recognize the peak aspect ratio and lowest orthogonal quality, the report quality is checked. We use the multiphase model because it has three phases: vapour, gas and liquid. In the solver settings, we used a transient pressure-based approach, and considered velocity in absolute terms. The energy equation is kept on. In the models, the volume of the fluid is enabled, the formulation is taken as implicit, and body force is also enabled. Three phases are taken and the type of phase can be defined in the options. Phase pairs can be defined in the 'phase attraction' and surface tension coefficients are also enabled. The options: continuum surface force, wall adhesion and jump adhesion are also kept on. Then, at the end of the multiphase model, we will set the mass transfer. After this, in the viscous option, the k–ε model is enabled as standard, enhanced wall treatment, thermal effect and curvature correction are also selected. Then, in the materials section, working fluids are selected which are acetone, acetone vapour and water in this case. Then, the properties of fluids like density, specific heat, thermal conductivity and viscosity are defined. The wall temperature and the filling ratio are defined in the CLPHP finally. The filling of fluid is shown below in the figures.

2.5. Basic settings for the domain

CLPHP is divided into three domains, i.e. the adiabatic region, condenser and evaporator. Furthermore, the adiabatic region is partitioned into two domains to encompass the rise in CLPHP from the evaporator at the base.

2.6. Boundary conditions

200 W and 300 W heat fluxes were applied to the evaporator region with 100, 200, 300 and 400 iterations. The heat flux is considered to be negligible for the adiabatic region. In the condenser region, a lower heat flux was given. The VOF model is utilized to obtain CFD results. In all domains, the no-slip condition is applied.

2.7. Condenser

In the condenser section, the velocity and relative pressure are negligible. Primarily, as there is only low-pressure air, there will be low turbulent flow in the condenser section. The volume fraction for the binary mixture of fluid and vapours is 0 while for air, it is 1. Upon completion of heating to the evaporator, the thermal boundary condition is applied with a fixed temperature of 302 K.

2.8. Evaporator

The same as in the condenser section, the velocity and relative pressure are negligible. In the evaporator, the values (0, 1, 0) are used to represent the vapour and the binary mixture of air and fluid. Across all domains, the no-slip condition is applied.

2.9. Material selection

The properties of the analysed fluids are listed in Table 2. For comparison, data for water are also given.

Table 2. Properties of fluid.

Fluid	Density, kg/m³	Specific heat, J/(kg·K)	Thermal conductivity, W/(m·K)	Dynamic viscosity, Pa·s
C_3H_6O	761	2160	0.18	0.000331
C_3H_6O - Vapour	2.37	2160	0.18	0.014
H_2O	998	4181	0.644	0.001003

3. Results and discussion

The filling ratio of the closed loop pulsating pipe is taken at 70%. The working fluids for this analysis are acetone and water. In this analysis, results are obtained by giving different heat inputs. Figure 6 shows the results obtained by applying a heat flux of 200 W after 100 iterations. Similarly, Fig. 7 shows the results after 200 iterations, Fig. 8 after 300 iterations, and Fig. 9 after 400 iterations, all with the same heat flux of 200 W. The vapour of acetone is illustrated in Fig. 10. Moving on, Fig. 11 presents the results for a heat flux of 300 W after 100 iterations. Figures 12, 13 and 14 show the results after 200, 300, and 400 iterations, respectively, with the same heat flux. The vapour of acetone is shown again in Fig. 15, and the final results are summarized in Fig. 16. The increment in the heat power input reduces the thermal resistance. While at low input of heat flux, enough perturbations are not generated and it results in the restriction of bubble pumping action. So, this phenomenon results in the poor performance. The heat transfer coefficient is improved with an enhancement in the heat input. Still, higher input heat fluxes resulted in bulk flow taking a fixed direction that did not reverse with time. This circulation was manifested as the adjacent tube became alternately hot and cold. Interestingly, in such a case the lowest thermal resistance was observed.

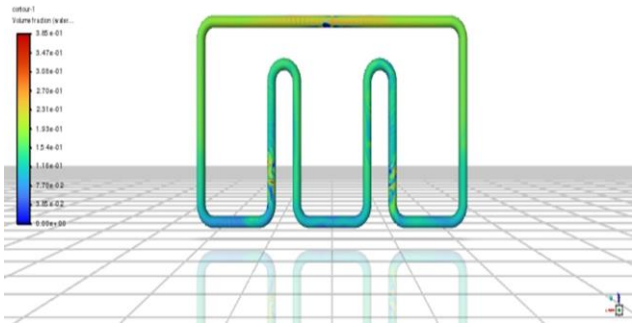

Fig. 6. Temperature contours at 200 W heat flux after 100 iterations for water-acetone.

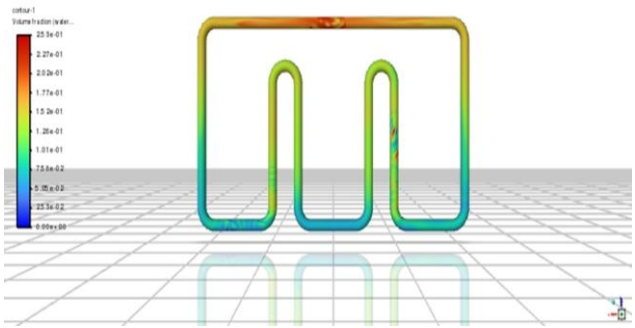

Fig. 7. Temperature contours at 200 W heat flux after 200 iterations for water-acetone.

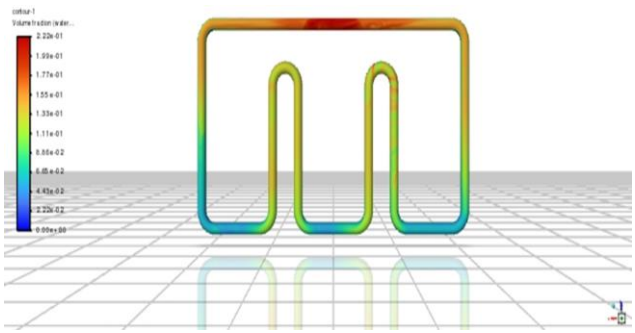

Fig. 8. Temperature contours at 200 W heat flux after 300 iterations for water-acetone.

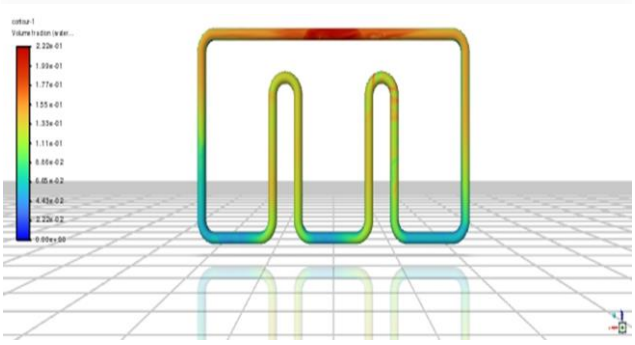

Fig. 9. Temperature contours at 200 W heat flux after 400 iterations for water-acetone.

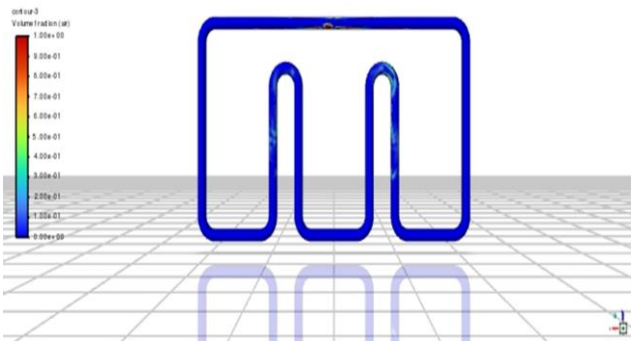

Fig. 10. Vapourized acetone at 200 W heat flux.

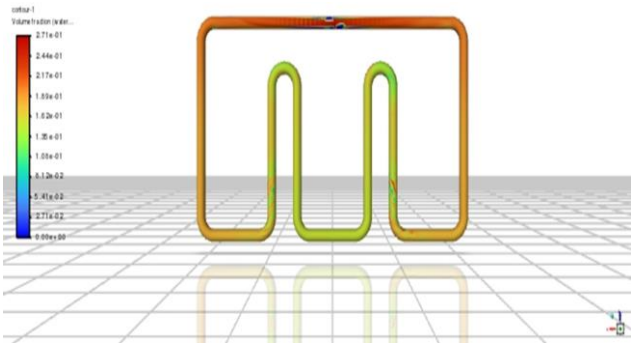

Fig. 11. Temperature contours at 300 W heat flux after 100 iterations for water-acetone.

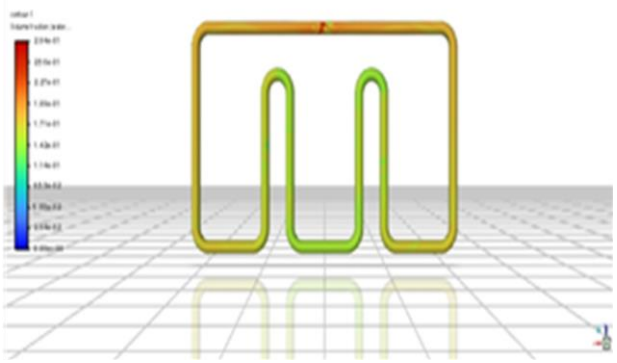

Fig. 12. Temperature contours at 300 W heat flux after 200 iterations for water-acetone.

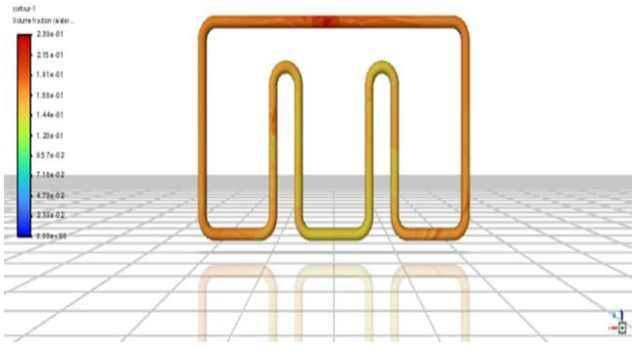

Fig. 13. Temperature contours at 300 W heat flux after 300 iterations for water-acetone.

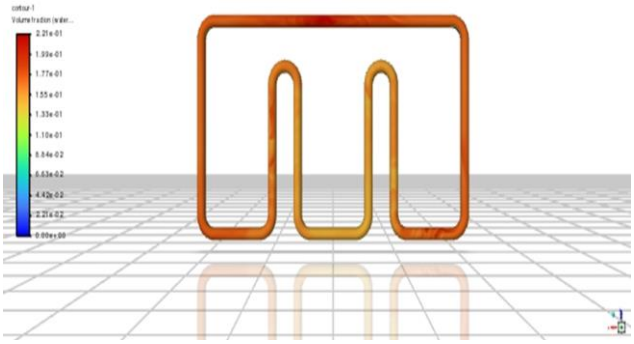

Fig. 14. Temperature contours at 300 W heat flux after 400 iterations for water-acetone.

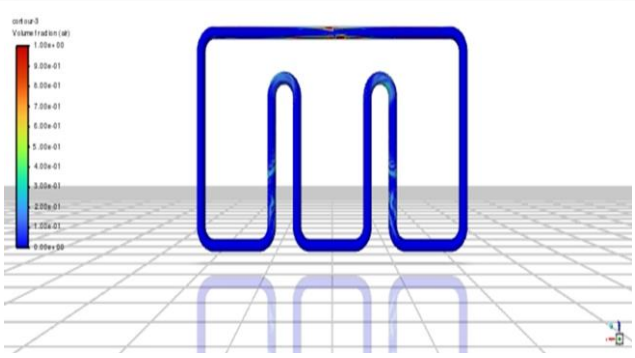

Fig. 15. Vapourized acetone at 300 W heat flux.

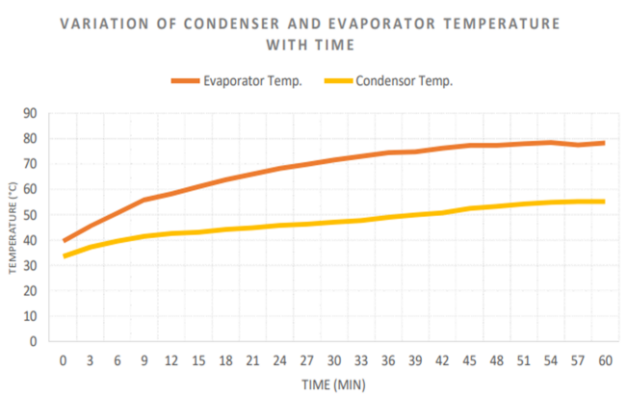

Fig. 16. Evaporator temperature and condenser temperature vs. time.

The above graph (Fig. 16) depicts the comparison of variations of evaporator and condenser temperature versus time. The temperature gradually enhances over time for both the condenser and evaporator. At the beginning of the heat transfer rate, the temperature rises gradually. Whenever the heat transfer rate increases, the rate of temperature rise decreases until it changes to a steady state which shows that it becomes constant. In the beginning, the difference between the condenser and evaporator temperature is lower and rises gradually. The optimum filling ratio for CLPHP in this study is 70%, which most adequately combines the advantages of the following two aspects: the latent heat along with the pumping action of the bubbles, and the sensible heat transport of the liquid slugs.

4. Conclusions

CFD analysis is used (ANSYS Fluent) to study the heat transfer characteristics of CLPHP. The working fluids are acetone and water. It is observed from the presented contours, as the time step size increases, the volume fraction of acetone-liquid decreases when the heat load is applied at the evaporator section. It was also observed that the acetone-liquid volume fraction decreases as the heat load increases in the CLPHP. This happens because the heat load increases at the evaporator section then the acetone-liquid to vapour phase transformation time is reduced. It is concluded that:

1. The thermal resistance and operating time of the PHP decrease as the heat input to the CLPHP increases.

2. If we apply more heat flux to the fluid, it cools down gradually. On the other hand, applying less heat flux causes it to cool more slowly.

3. When heat flux is applied to the evaporator, less heat is transferred to the condenser compared to the evaporator. Over time, the temperature in the condenser stabilizes and becomes nearly constant.

4. As shown in Fig. 16, at T=0, the evaporator's temperature is around 40°C, while the condenser's temperature is about 32°C. After 18 minutes, the evaporator's temperature rises to 62°C, and that of the condenser reaches approximately 43°C. By 60 minutes, the evaporator heats up to around 79°C, and the condenser reaches about 55°C.

5. From these observations, it is clear that the evaporator's temperature increases more significantly over time compared to the condenser's temperature.

6. In the future, this study can be expanded by exploring variations in the filling ratios and introducing additional parameters like the Grashof and Prandtl numbers.

References

[1] Akachi, H. (1990). *Structure of heat pipe*. U.S. Patent 4 921 041.

[2] Suresh, Z.V., & Bhramara, B. (2016). CFD Analysis of single turn pulsating heat pipe. *International Journal of Scientific and Engineering Research*, 7(6), 238−244.

[3] Wang, J., Xie, J., & Liu, X. (2019). Investigation on the performance of closed-loop pulsating heat pipe with surfactant. *Applied Thermal Engineering*, 160, 113998. doi:10.1016/j.applthermaleng.2019.113998

[4] Reddy, D.R., Reddy, K.H., & Balajiganesh, N. (2017). Performance Analysis of Pulsating Heat Pipes Using Various Fluids. *International Journal of Engineering and Manufacturing Science*, 7(2), 281−291.

[5] Girish, S., Lavanya, K., & Krishna, P.G. (2017). CFD analysis of Pulsating heat pipe using different fluids. *International Journal of Mechanical Engineering and Technology*, 8(6), 804-812.

[6] Rudresha, S., Goyal, P., Pandey, P., Sharma, M., & Srivastav, M. (2021). CFD Analysis of Single Turn Pulsating Heat Pipe by Comparing Ethylene Alcohol & Water. *International Journal of Mechanical Engineering and Technology*, 8(7), 2273−2279.

[7] Betancur, L., Mangini, D., Mantelli, M., & Marengo, M. (2020). Experimental study of thermal performance in a closed loop pulsating heat pipe with alternating superhydrophobic channels. *Thermal Science and Engineering Progress*, 17, 100360. doi: 10.1016/j.tsep.2019.100360

[8] Li, C., & Li, J. (2021). Passive Cooling Solutions for High Power Server CPUs with Pulsating Heat Pipe Technology. *Frontiers in Energy Research*, 9. doi: 10.3389/fenrg.2021.755019

[9] Haque, M.M.A., Azizuddin, D.M., & Rehman, M.M.K. (2016). CFD and Volume Fraction Analysis of Closed Loop Pulsating Heat Pipe (CLPHP). *Journal of Mechanical and Civil Engineering*, 13(5), 88–94. doi: 10.9790/1684-1305048894

[10] Xue, Z.H., & Qu, W. (2017). Experimental and theoretical research on an ammonia pulsating heat pipe: New full visualization of flow pattern and operating mechanism study. *International Journal of Heat and Mass Transfer*, 106, 149−166. doi: 10.1016/j.ijheatmasstransfer.2016.09.042

[11] Pachghare, P.R., & Mahalle, A.M. (2013). Effect of pure and binary fluids on closed loop pulsating heat pipe thermal performance. *Procedia engineering*, 51, 624−629. doi: 10.1016/j.proeng.2013.01.088

[12] Baitule, D.A., & Pachghare, P.R. (2013). Experimental analysis of closed loop pulsating heat pipe with variable filling ratio. *International Journal of Mechanical Engineering and Robotic Research*, 2(3), 113−121.

[13] Patel, V.M., & Mehta, H.B. (2016). Influence of Gravity on the Performance of Closed Loop Pulsating Heat Pipe. *18th International Conference on Fluid Mechanics and Thermal*., 12−13 Jan., 18(1), Part V. Zurich, Switzerland. *International Journal of Mechanical and Mechatronics Engineering*, 10(1), 219−223.

[14] Yeswanth, A., & Bhaskara Rao T.S.S. (2016). CFD Analysis on pulsating heat pipe to improve heat transfer. *International Journal of Research and Innovation in Thermal Engineering*, 3.1, 107−111.

[15] Rahman, M.L., Kader, M.F., Rahman, M.Z., & Ali, M. (2016). Experimental investigation on thermal performance of a closed loop pulsating heat pipe without fin and with fin structure. *American Journal of Mechanical Engineering*, 4(6), 209−214. doi: 10.12691/ajme-4-6-1

[16] Pachghare, P.R., & Mahalle, A.M. (2014). Thermohydro-dynamics of closed loop pulsating heat pipe: an experimental study. *Journal of Mechanical Science and Technology*, 28(8), 3387−3394. doi: 10.1007/s12206-014-0751-9

[17] Sree, N.S., Sudheer, N.V.S.S., & Bhramara, P. (2018). Thermal analysis of closed loop pulsating heat pipe. *International Journal of Mechanical and Production Engineering Research and Development*, 8(2), 21−36. doi:10.24247/ijmperdapr20183

[18] Yang, H., Khandekar, S., & Groll, M. (2008). Operational limit of closed loop pulsating heat pipes. *Applied Thermal Engineering*, 28(1), 49−59. doi: 10.1016/j.applthermaleng.2007.01.033

[19] Khandekar, S., Charoensawan, P., Groll, M., & Terdtoon, P. (2003). Closed loop pulsating heat pipes Part B: visualization and semi-empirical modeling. *Applied Thermal Engineering*, 23(16), 2021−2033. doi: 10.1016/S1359-4311(03)00168-6

[20] Khandekar, S., & Groll, M. (2004). An insight into thermo-hydrodynamic coupling in closed loop pulsating heat pipes. *International journal of thermal sciences*, 43(1), 13−20, doi: 10.1016/S1290-0729(03)00100-5

[21] Xu, J.L., Li, Y.X., & Wong, T.N. (2005). High speed flow visualization of a closed loop pulsating heat pipe. *International Journal of Heat and Mass Transfer*, 48(16), 3338−3351. doi: 10.1016/j.ijheatmasstransfer.2005.02.034

[22] Khan, M.N., & Nadeem, S. (2020). Theoretical treatment of bioconvective Maxwell nanofluid over an exponentially stretching sheet. *Canadian Journal of Physics*, 98(8), 732−741. doi: 10.1139/cjp-2019-0380

[23] Khan, M.N., Ahmad, S., Alrihieli, H.F., Wang, Z., Hussien, M.A., & Afikuzzaman, M. (2023). Theoretical study on thermal efficiencies of Sutterby ternary-hybrid nanofluids with surface catalyzed reactions over a bidirectional expanding surface. *Journal of Molecular Liquids*, 391, 123412. doi: 10.1016/j.molliq.2023.123412

[24] Khan, M.N., Nadeem, S., & Muhammad, N. (2020). Micropolar fluid flow with temperature-dependent transport properties. *Heat Transfer*, 49(4), 2375−2389. doi: 10.1002/htj.21726.

[25] Khan, M.N., Hussien, M.A., Allehiany, F.M., Ahammad, N.A., Wang, Z., & Algehyne, E.A. (2023). Variable fluid properties and concentration species analysis of a chemically reactive flow of micropolar fluid between two plates in a rotating frame with cross diffusion theory. *Tribology International*, 189, 108943. doi: 10.1016/j.triboint.2023.108943

[26] Ahmad, S., Khan, M.N., & Nadeem, S. (2020). Mathematical analysis of heat and mass transfer in a Maxwell fluid with double stratification. *Physica Scripta*, 96(2), 025202. doi: 10.1088/1402-4896/abcb2a

[27] Khan, M.N., Ahmed, A., Ahammad, N.A., Wang, Z., Hassan, A.M., & Elkotb, M.A. (2023). Chemotaxis bioconvection in swirling flow of Maxwell fluid with diffusion-thermo and thermal-diffusion effects. *Case Studies in Thermal Engineering*, 49, 103334. doi: 10.1016/j.csite.2023.103334

[28] Ahsan, N., Nauman Aslam, M., Khan, M.N, & Elseesy, I.E. (2023). Thermal features of Darcy-Forchheimer on a micropolar fluid flow over a curved stretching surface with homogenous-heterogeneous reactions. *Numerical Heat Transfer A*, 1−15. doi: 10.1080/10407782.2023.2251082

[29] Khan, M.N., Khan, A.A., Wang, Z., Alrihieli, H.F., M. Eldin, S., Aldosari, F.M., & Elseesy, I.E. (2023). Flow investigation of the stagnation point flow of micropolar viscoelastic fluid with modified Fourier and Fick's law. *Scientific Reports*, 13(1), 9491. doi: 10.1038/s41598-023-36631-1

[30] Ju, M., Li, B., Wu, Y., Wang, Z., Sun, Z., Zhan, S., & Wang, J. (2023). Oil droplet migration in the coupling of electric field and nano-confined shearing flow field: A molecular dynamics study. *Journal of Molecular Liquids*, 388, 122813. doi: 10.1016/j.molliq.2023.122813

[31] Khan, M.N., Ahmad, S., Wang, Z., Ahammad, N.A., & Elkotb, M.A. (2023). Bioconvective surface-catalyzed Casson hybrid nanofluid flow analysis by using thermodynamics heat transfer law on a vertical cone. *Tribology International*, 188, 108859. doi: 10.1016/j.triboint.2023.108859

[32] Khan, M.N., Ahmed, A., Ahammad, N.A., Wang, Z., Hassan, A.M., & Elkotb, M.A. (2023). Chemotaxis bioconvection in swirling flow of Maxwell fluid with diffusion-thermo and thermal-diffusion effects. *Case Studies in Thermal Engineering*, 49, 103334. doi: 10.1016/j.csite.2023.103334

[33] Tian, J., He, C., Chen, Y., Wang, Z., Zuo, Z., Wang, J., & Xiong, J. (2024). Experimental study on combined heat transfer enhancement due to macro-structured surface and electric field during electrospray cooling. *International Journal of Heat and Mass Transfer*, 220, 125015. doi: 10.1016/j.ijheatmasstransfer.2023.125015

[34] Khan, M.N., Haider, J.A., Wang, Z., Gul, S., Lone, S.A., & Elkotb, M.A. (2024). Mathematical modelling of the partial differential equations in microelectromechanical systems (MEMS) and its applications. *Modern Physics Letters B*, 38(05), 2350207. doi: 10.1142/S021798492350207X

[35] Khan, M.N., Aldosari, F.M., Wang, Z., Yasir, M., Afikuzzaman, M., & Elseesy, I.E. (2024). Overview of solar thermal applications of heat exchangers with thermophysical features of hybrid nanomaterials. *Nanoscale Advances*, 6(1), 136−145. doi: 10.1039/D3NA00481C

[36] Giri, K.C., & Pachghare, P. R. (2021). Study of Thermal Performance of Closed Loop Pulsating Heat Pipe using Computational Fluid Dynamics. *International Journal for Research in Applied Science and Engineering Technology*. 9(9), 1384−1388. doi: 10.22214/ ijraset.2021.38088